

Designing an electric motorcycle for the Isle of Man TT Zero race, and how electric vehicle racing could be used to spur innovation

Lennon Rodgers¹, Radu Gogoana, Thomas German,
Mark Jeunette, Randall Briggs, Erick Fuentes, Will Pritchett
¹*Massachusetts Institute of Technology, Cambridge, MA, USA, rodgers@alum.mit.edu*

Abstract

This paper describes the process of designing, building, and racing a high performance electric motorcycle for the 2011 Isle of Man Tourist Trophy (TT) Zero race. The TT race is the oldest existing motorcycle race (est. 1907), and is known for high speeds, over 200 sharp turns, and danger to the rider. These demands created a challenge to engineer a machine that was capable of finishing the entire course on a single battery charge in the fastest time possible. The design process consisted of systems engineering, subsystem design, final system design, testing, and model validation. Simulations were useful for understanding how the design parameters affect performance metrics. “Full throttle” simulations were performed to estimate the maximum acceleration, speed, and power of the motorcycle. To estimate the energy required to traverse the entire course, it is necessary to make assumptions about the throttle profile, speed, or power. Since it was difficult to predict the throttle profile for the entire race, both constant speed and constant power drive cycles were assumed. The electrical and mechanical designs of the motorcycle used mostly off-the-shelf components, though custom designs were generated for the instrumentation, motor shaft and structural frame that housed the motors and batteries. Real-time sensing provided a rich data set that was used to validate the models; it was found that the models were able to predict the acceleration, maximum speed, and energy consumption to within 5% of the actual values.

Finally, guidelines for designing innovative zero emission races were presented and described. In this paper innovation was defined as the act of generating a product or service that (1) reduces the environmental impact of vehicles and (2) consumers want to purchase. The guidelines suggest to consider the historical context, utilize the power of regulation, drive technology, provide valued entertainment, and inspire consumer demand.

Keywords: electric motorcycle, design, modeling, EV, zero emission racing

1 Introduction

For over 100 years the Isle of Man Tourist Trophy (TT) race has served as a proving ground for both riders and engineers to push the envelope of motorcycle technology. Soichiro Honda, founder and then president of Honda Motor Corporation, once declared that the innovation required to win the Isle of Man race would “rank at the world’s highest levels of engineering.” [1] The desire for innovation through racing continues today, and in 2009 an electric class was added to the TT with the aim of advancing zero emission vehicle technology.

The TT race course is 60.73 km long, both urban and mountainous, held on public roads, and circles the entire island [2]. The demands of the course created a challenge to engineer a machine that was capable of handling sharp turns at high speeds and finish the entire course on a single battery charge in the fastest time possible.

This paper will describe the process of designing, building and racing a high performance electric motorcycle for the 2011 TT. The design process can be grouped by systems engineering (Section 2), detailed design (Section 3), and model validation (Section 4). This work builds upon previous vehicle modeling research [3][4].

2 Systems Engineering

A vehicle can be thought of as a complex system whose individual components (i.e. subsystems) can be better understood through mathematical models. The individual models should provide insight into the fundamental functions of each subsystem, and reveal the basic design trade-offs that exist. The various subsystem models can be combined to produce a system model of the entire vehicle, and thus allow for specific design decisions to be explored through parameter variation. In the case of an electric vehicle (EV), it is often of interest to explore performance metrics such as acceleration, speed, and range. These performance metrics can only be explored through a system model, since they are coupled with design parameters such as battery capacity, motor size, mass, aerodynamics, and gear ratio(s). This type of systems engineering is most useful in the early stages of design and aids in finalizing subsystem level requirements. In practice it is difficult to finalize all of the requirements early in the design process, thus

systems engineering is also useful in later design stages for further trade-offs studies.

The intent of this section is to describe how system-level engineering was used in designing the electric motorcycle. More specifically, it is of interest to explain the methods used to explore how changes in the *design parameters* affect *performance metrics* (Table 1). To fulfill this objective, derivations of subsystem and system models are included (Section 2.1). These models will be used to simulate the motorcycle performance when the throttle profile is specified (Section 2.2). This method is useful for estimating power, acceleration and speed when “full throttle” is applied. However, it is uncommon to know the throttle profile for the entire course, thus Section 2.3 will derive a method for estimating performance metrics based on assumed rider behavior (i.e. drive cycles). This method is useful when estimating the energy required to traverse the course, average speed, and time to finish.

Table 1: Design parameters and performance metrics.

Design Parameters	Performance Metrics
<ul style="list-style-type: none">• Battery capacity• Maximum and continuous power of motor• Mass• Aerodynamics• Rolling resistance• Gear ratio	<ul style="list-style-type: none">• Acceleration• Maximum and average speed• Distance travelled on a single charge

2.1 Subsystem models

An electric motorcycle can be decomposed into the following four subsystems: vehicle, motor, motor controller, and battery. Models for each of these subsystems will now be derived.

The approach was to first derive a mathematical relationship for the acceleration of the vehicle, \ddot{x} , and the force from the drive wheel, F_w . These values were then numerically integrated to determine the speed (\dot{x}) position (x), and power at the driven wheel (P_w):

$$\dot{x}_{i+1} = \dot{x}_i + \ddot{x}_i(t_{i+1} - t_i) \quad (1)$$

$$x_{i+1} = x_i + \dot{x}_{i+1}(t_{i+1} - t_i) \quad (2)$$

$$P_{w,i} = F_{w,i}\dot{x}_i \quad (3)$$

The motorcycle was modeled as a mass on an incline with externally applied forces (Figure 1) [5]. It is propelled forward by an electric motor acting through the rear wheel with a force, F_w , but slowed down by the aerodynamic drag, F_{aero} , the rolling resistance from the wheels, $F_{rolling}$, and the

horizontal component of weight, F_{gravity} . Thus the acceleration can be written as [6]:

$$\ddot{x} = \frac{1}{m} (F_w - 1/2 \rho C_d A (\dot{x} + w)^2 - mg C_{rr} \cos \beta - mg \sin \beta) \quad (4)$$

Where m is the total mass of the motorcycle and rider, w is the wind speed, C_{rr} is the rolling resistance coefficient, ρ is the density of air, $C_d A$ is the aerodynamic coefficient, g is gravity, and β is the angle of the road.

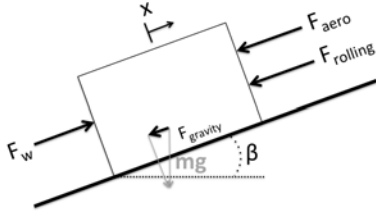


Figure 1: Motorcycle model.

The next objective is to determine a relationship for the force on the rear wheel, F_w . The motor torque (τ_m) acts through a chain and two sprockets to produce the force on the rear wheel. Using conservation of power:

$$F_w = \frac{\eta_d z \tau_m}{r_w} \quad (5)$$

Where z is the gear ratio and η_d is the efficiency for the sprocket-chain drivetrain. This equation assumes that the wheel has no rotational inertia.

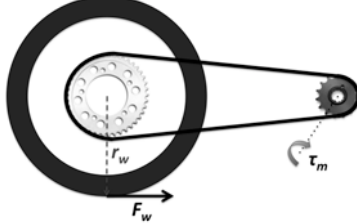


Figure 2: A free body diagram of the drivetrain.

For a DC permanent magnet motor, the motor torque is proportional to the current passing through the motor (I_m):

$$\tau_m = K_\tau I_m \quad (6)$$

Where K_τ is the torque constant, and is specified in the motor datasheet. The motor receives power from the motor controller, which outputs V_m and I_m based on the throttle command. If the throttle is held constant then I_m is held constant. If “full throttle” is applied then the maximum amount of current is output continuously, I_m^{limit} ¹. However, this is only true at certain speeds and the reason can be explained through a motor model. The motor can be modeled as a voltage-generating source (V_{emf}) in series with a resistor (R_m) (Figure

3). By summing the voltages around the motor model circuit, the following relationship can be derived:

$$I_m = (V_m - V_{\text{emf}})/R_m \quad (7)$$

V_{emf} is proportional to the rotational speed of the motor, $\dot{\theta}_m$, which is related to the linear speed of the rear wheel, \dot{x} , since they are connected. Rewriting Equation (7):

$$I_m = \frac{V_m - K_\theta \dot{\theta}_m}{R_m} = \frac{V_m - K_\theta \frac{z}{r_w} \dot{x}}{R_m} \quad (8)$$

Figure 3: Model of a DC PM motor.

As shown in Equation (8), as \dot{x} increases, the motor controller must continually increase V_m to maintain a constant I_m output. However, the motor controller can only increase V_m to equal the battery voltage, V_b . When $V_m = V_b$, I_m begins to decrease as shown in Figure 4 as a solid line. Thus:

$$I_m = \min \left\{ s I_m^{\text{limit}}, \frac{V_b - K_\theta \frac{z}{r_w} \dot{x}}{R_m} \right\} \quad (9)$$

The variable s is the throttle signal, which can vary from 0 to 1.

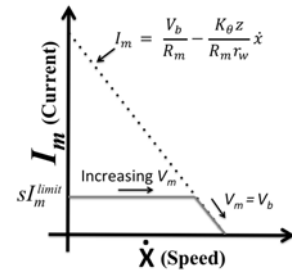


Figure 4: Current-speed curve of the motor.

The battery voltage, V_b , depends on the current being drawn from the battery, I_b . A single battery cell can be modeled as a voltage source and a resistor, R_c (Figure 5). Battery cells are combined in series (k) and parallel (l) to obtain the desired voltage and capacity. The total resistance of the battery pack can be written as:

$$R_b = \frac{k}{l} R_c \quad (10)$$

The pack voltage during discharge can be determined using Ohm's law:

$$V_b = V_b^n - I_b R_b \quad (11)$$

Where V_b^n is the voltage on the battery pack when no current is being drawn.

¹ I_m^{limit} is assigned in the motor controller software.

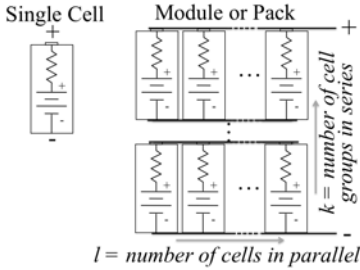


Figure 5: Model of a battery pack.

The battery current can be determined by modeling the motor controller with the battery and motor (Figure 6). Power is conserved through the motor controller, thus:

$$I_b = \frac{V_{m,l}^n}{\eta_{mc} V_b} \quad (12)$$

Where η_{mc} is the efficiency of the motor controller. Combining Equations (11) and (12) yields an equation that can be solved for I_b :

$$\eta_{mc} R_b I_b^2 - \eta_{mc} V_b^n I_b + V_m I_m = 0 \quad (13)$$

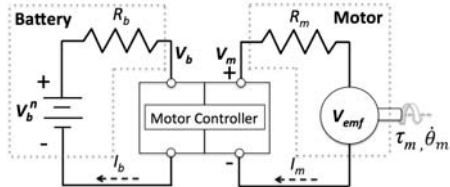


Figure 6: Combined power electronics model.

Finally, the power from the motor can be related to Equation (3):

$$P_{m,i} = P_{w,i} / \eta_d \quad (14)$$

And the energy from the battery can be calculated using:

$$E_{b,i} = V_{b,i} I_{b,i} (t_{i+1} - t_i) \quad (15)$$

2.2 Simulations based on a known throttle input

The methods described in this subsection can be used to explore trade-offs between design parameters and performance metrics (Table 1) when the throttle input, s_i , is specified as a function of distance or time. For example, it is often of interest to understand how the gear ratio will affect the maximum speed and acceleration. One useful method is to assume a “step input,” which would simulate the rider applying “full throttle” ($s_i = 1$). Any other specified throttle input profile could also be used (saw tooth, etc.). Thus the following algorithm can be used for estimating the state of the motorcycle based on a known throttle profile:

1. Obtain the throttle profile (e.g. $s_i = 1$ for full throttle) and calculate $I_{m,i}$ using Equation (9), and then the motor torque using Equation (6).
2. Calculate the wheel force ($F_{w,i}$) using Equation (5), obtain a road angle (β_i) from the GPS data, and use Equation (4) to calculate the vehicle acceleration (\ddot{x}_i).
3. Calculate the power and energy values using Equations (3), (14), and (15).
4. Use Equations (1) and (2) to step forward in time ($i+1$). Repeat the algorithm for the next increment.

The main limitation of the algorithm described above is the difficulty in knowing the throttle input, s_i , as a function of distance or time. It is typically infeasible to know the throttle profile for the entire course, since the rider adjusts the throttle in real-time based on personal judgment. Thus this algorithm is not often used to estimate the battery energy required to traverse the *entire* course. However, it is useful in exploring maximum power, acceleration and speed during short “full throttle” simulations.

Full throttle simulations show how maximum acceleration and speed largely depend on the drag forces (e.g. sum of the gravity, rolling, and aero forces) and the motor output power. The motor power that is in excess of the drag power causes the vehicle to accelerate. As the motorcycle increases in speed, the drag forces increase as shown in Figure 7. The motor has a constant torque until the back-emf becomes limiting, which is when the available power from the motor starts to decrease. Once the motor and drag power are equal, the vehicle no longer accelerates and this represents the maximum speed. Thus the intersection of the motor and drag power curves is the maximum speed of the motorcycle, and where the vehicle’s acceleration is zero.

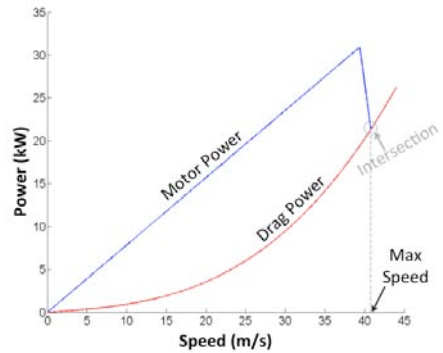


Figure 7: Simulation of power versus speed.

The behavior of the motor power curve is heavily influenced by both the gear ratio and the maximum current from the motor controller (I_{limit}).

A larger gear ratio and/or I_{limit} will yield higher motor power at a given speed, and thus greater acceleration (Figure 8 and Figure 9). However, increasing the gear ratio decreases the maximum speed. Simulations can be used to select the appropriate current limit and gear ratio.

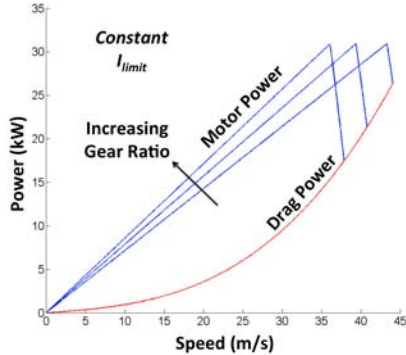


Figure 8: Simulation of power versus speed.

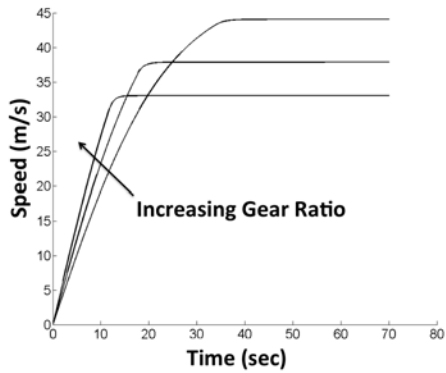


Figure 9: Simulation of speed versus time.

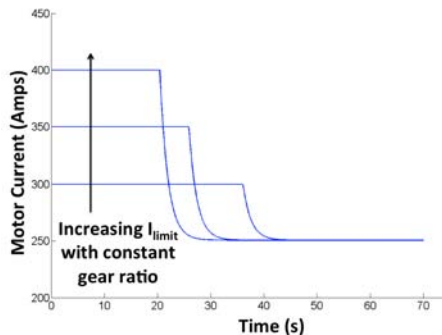


Figure 10: Simulation of motor current versus time.

The motor controller limits the amount of current to the motor (I_{limit}), and the motors will overheat if too much continuous current is applied for too long. Thus over heating is the main consideration when selecting the proper motor controller settings. Motors are specified as having a continuous and short-burst (peak) rating, though there are many complicating factors (e.g. air cooling) that prevent certainty in how long the short-burst can be operated. Even

the continuous rating often has various assumptions. As shown in Figure 10, more current is needed during vehicle acceleration than at steady state/cruise conditions. This is because the motor becomes back-emf limited.

2.3 Simulations based on an assumed drive cycle

Driving behavior has a huge impact on the average speed and energy estimates. Driving more aggressively will increase both the power and energy requirements. The algorithms described in Section 2.2 capture the rider behavior through the variable s (see Equation (9)), though in reality it is very difficult to know exactly how the throttle will be varied over the entire course. A “drive cycle” specifies the speed or power versus time or distance, along with the corresponding GPS coordinates of the route, and thus acts to describe the rider behavior.

The GPS coordinates of the course were obtained for the TT race, but no additional drive cycle information was known. The race course is quite complex with over 200 turns and continuous changes in elevation. With limited information, broad assumptions were made to estimate an appropriate drive cycle. Thus two drive cycles were assumed: (1) The first assumed that the vehicle maintains a constant speed throughout the course. A constant speed assumption will yield an underestimate for battery energy use since it is most energy efficient to maintain a constant speed. (2) The second drive cycle assumed the vehicle maintains a constant motor power. This is likely an over estimate of energy use since driving at constant power will yield large speed fluctuations, which is an inefficient way of using energy.

The estimate so far has not included the energy losses that occur during braking, which will increase the estimates for the energy used, and decrease the average speed. One method is to define a “braking efficiency”, χ , as:

$$\chi \equiv \frac{\text{avg. speed with braking}}{\text{avg. speed without braking}} \quad (16)$$

For example, it can be assumed that the braking reduces the average speed by 15%, thus $\chi=0.85$. The average speed, \bar{x} , when braking is included can now be written as:

$$\bar{x}^B = \chi \bar{x} \quad (17)$$

where the superscript “B” denotes values after braking estimates are included. The time to finish the course x_{finish} will be increased by Δt^B :

$$t_{\text{finish}}^B = t_{\text{finish}} + \Delta t^B \quad (18)$$

which can also be written as:

$$\begin{aligned}\Delta t^B &= \frac{x_{\text{finish}}}{\chi \bar{x}} - \frac{x_{\text{finish}}}{\bar{x}} \\ &= \frac{x_{\text{course}}}{\bar{x}} \left(\frac{1}{\chi} - 1 \right) = t_{\text{finish}} \left(\frac{1}{\chi} - 1 \right)\end{aligned}\quad (19)$$

By combining Equations (18) and (19) yields the new time to finish:

$$t_{\text{finish}}^B = \frac{t_{\text{finish}}}{\chi} \quad (20)$$

For the constant power drive cycle, the motors would have to operate at a constant power for the additional time, Δt^B , thus:

$$E_b^B = P_m t_{\text{finish}}^B = \frac{P_m t_{\text{finish}}}{\chi} = \frac{E_b}{\chi} \quad (21)$$

Using the assumed drive cycles, Equations (1) through (4), (14), (15) and (21) were used with GPS data to estimate the power from the motors, energy from the batteries, and average speed.

2.4 Estimating the capacity of the battery and power of the motor

It is critical to determine if the general design requirements can be met given the constraints of technology, time and budget. In the case of the motorcycle race, the objective was to finish the entire course within a competitive time. However, technological limitations such as battery energy density or motor power could severely constrain the design or make it infeasible. This subsection describes how the methods in Section 2.3 were used to estimate the required motor power and battery capacity and determine if the appropriate motors and batteries are available that could fit within the volumetric limitations of a motorcycle.

The first step was to calculate the average speed based on the desired finish time:

$$\bar{x} = \frac{x_{\text{finish}}}{t_{\text{finish}}} \quad (22)$$

where x_{finish} is the known distance of the course. Once the desired average speed is known, this value can be used to estimate the battery energy and motor power required to traverse the course given a constant speed drive cycle. Next, the equations for a constant power drive cycle were entered into a parametric spreadsheet, and the constant power value was varied until the same average speed was obtained. This ensures that a fair comparison is being made with both the constant speed and constant power drive cycles.

For the final estimates, it was assumed that an average speed of 137 km/h (27 minutes) would be competitive, which based on the drive cycle estimations would required 22 kW of

average power from the motors and ~10 to 11 kWh of battery energy (Figure 11). The braking constant, χ , was assumed to be 0.8 for the constant power drive cycle and 0.82 for the constant speed drive cycle. The corresponding volume of the batteries and motors were modeled in CAD to ensure adequate space on the motorcycle chassis (Figure 12). Note that lean angle and ground clearance surfaces were added to the CAD. The battery and motor masses were also calculated and included within an overall mass budget.

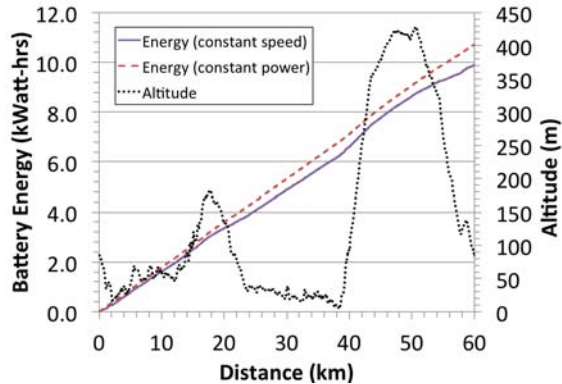


Figure 11: Simulation of the battery energy consumed during the race assuming a 137 km/h average speed.

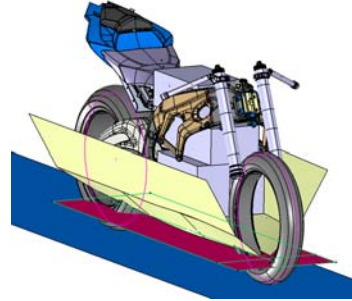


Figure 12: CAD was used to ensure sufficient volume for the batteries and motors.

3 Final Design

A 2010 BMW S1000RR motorcycle was used as the base chassis. The CAD of the final design is shown in Figure 18, and the component specifications are listed in Table 2. This section will describe the electrical (Section 3.1) and mechanical designs (Section 3.2), along with the methods used for testing (Section 3.3).

3.1 Electrical design

Due to cost, availability, volume, and mass constraints, it was decided to use two DC, permanent magnet, air-cooled motors from Lynch Motor Company. The motor selection set the maximum voltage on the battery pack to ~100V. The battery pack was designed with help from

A123 Systems; a customized version of their prismatic lithium-ion Nanophosphate® modules were used. A single motor controller from Kelly Controls was used to regulate the energy to both motors.

The motorcycle was instrumented with sensors to measure acceleration, speed, location (GPS), current, voltage, and temperature. A battery management system (BMS) was used to measure the voltage of each cell and perform cell balancing. A safety monitoring system from A123 Systems checked for vitals such as ground faults, the condition of the fuse, and over current. All of the sensing was integrated via a CAN-bus and an open-source microcontroller made by Arduino.

The data was transmitted to a laptop via xBee wireless transmitters/receivers. The data was displayed off-board in real-time via a Graphical User Interface (GUI) written in an open-source environment by Processing.org, and also logged on-board for post-race analysis. The rider display consisted of a series of simple LEDs to indicate the state of the motorcycle and warnings. Also, a single LCD screen was used to display digital values for power, energy consumed and speed.

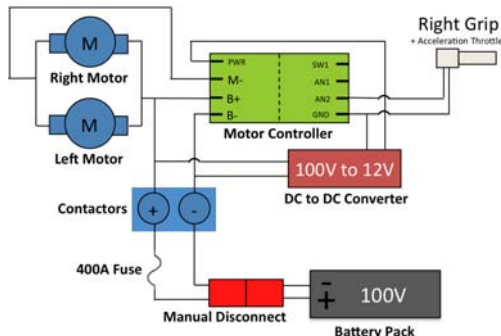


Figure 13: Wiring diagram of the motorcycle's power electronics.

3.2 Mechanical design

The entire motorcycle was designed in CAD, which enabled the various subsystems to fit inside the motorcycle with ~ 0.5 millimeter accuracy.² A structural frame was needed to support the batteries, motor, and supporting electronics; the removal of the engine needed to be considered in the mechanical design, since it was originally a structural element (Figure 14). Instead of a more common space-frame weldment, it was decided to design a frame that

² CAD of the S1000RR chassis was provided by BMW.

could be made purely on the waterjet using aluminum plates. The waterjet was chosen because it is rapid, economical, and provides significant design flexibility. The final frame design is shown in Figure 15. Designing a set of 2D plates also made prototyping easy; a laser cutter, wood and cardboard were used to quickly prototype various designs. The frame was assembled like a puzzle piece, with small tabs connecting the various 2-D plates together. The frame, including the tab-slots, was welded while bolted in place on the motorcycle chassis. A rigid steel jig was made to preserve the proper spacing and parallelism for the motors during welding. It should also be noted that an integrated design was used to house both the motors and batteries in one weldment assembly.

The motors were connected via a custom designed drive shaft (Figure 16). Finite Element Analysis was used to ensure that the shaft could handle the maximum torque loads of the motors and chain. Typically there is a flexible element in the drive shaft to provide compliance for misalignment, though in this case it was assumed that the flexure in the frame mounting was sufficient.³

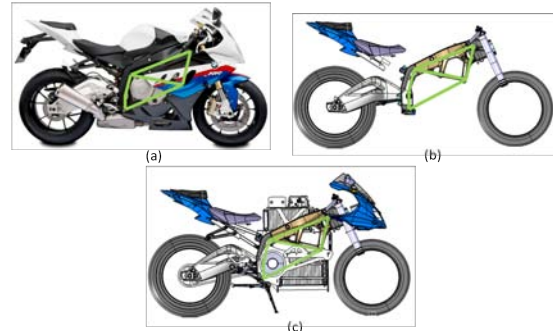


Figure 14: The structural loop needed to be preserved when the engine was replaced by batteries and motors.

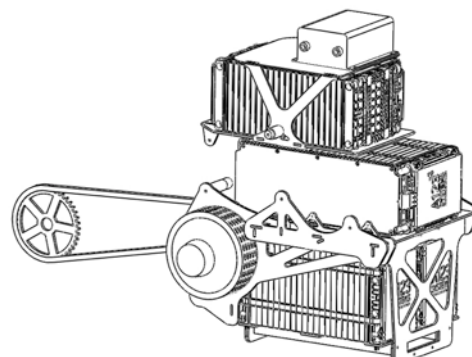


Figure 15: Final design of the battery and motor structural frame (shown with motors and batteries).

³ Based on a discussion with the motor designer (Cedric Lynch).

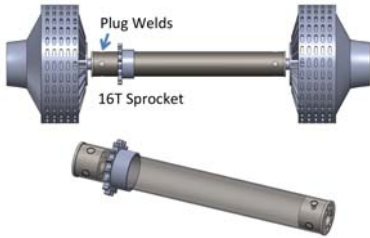


Figure 16: The motors were connected together with a rigid shaft.

3.3 Testing

A series of incremental tests were performed to ensure that each subsystem operated as predicted. This included the following tests: bench-top, wind tunnel, chassis dynamometer, track, and finally road. The methods, results and usefulness of these tests will be the focus of this subsection.

Bench-top tests were performed to ensure that each subsystem was functioning as expected before it was integrated into the rest of the motorcycle. The motorcycle chassis, main fairings, and cardboard mock-ups of the batteries and motors were assembled and tested in the MIT wind tunnel. This aided in estimating the aerodynamic coefficient.

The fully assembled motorcycle was then tested extensively (20+ hours) on a chassis dynamometer. These tests were intended to ensure that the drivetrain and other components were able to withstand full load and speed, match the current going to each motor, understand the thermal characteristics of the batteries and motor, validate and tune the analytical models, and measure the drive-train efficiency. Figure 17 shows how the dynamometer was used to tune and validate the motorcycle models derived in Section 2.

Track tests were performed at New Hampshire Motor Speedway, where the motorcycle was brought to maximum speed for prolonged periods of time. The motorcycle was then sent by air from Boston to the Isle of Man inside a wooden crate. Partial disassembly was required, since import/export regulation required the batteries to be shipped separately by the manufacturer (A123 Systems). The motorcycle was reassembled on the Isle of Man, and a dynamometer was used to run the motorcycle under full load and speed. Finally, the motorcycle was road-tested on the Isle of Man before the races.

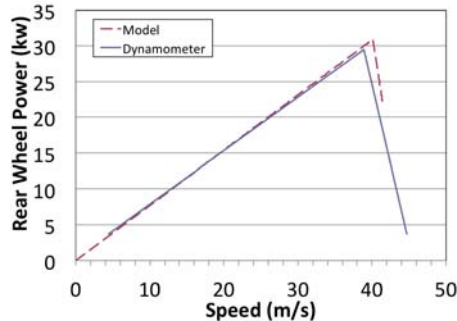


Figure 17: Dynamometer data with model predictions of the power output at the rear wheel.



Figure 18: CAD of the final design.

Table 2: Final component specifications.

Masses			
Rolling Chassis	Battery Modules	Motors	Other
77kg	106kg	25kg	23kg
Mass Distribution			
Front Wheel	Rear Wheel	Total Mass	
122kg	109kg	231kg	
Battery Specifications			
Paral./series	Voltage	Capacity	
6/30	99V	11.88 kWh	
Motor Specifications (2 motors combined)			
Power	Cont. Current	Model Number	
32 kW	400A	D135RAG	
Motor Controller Specifications			
Voltage	Cont. Current	Model Number	
18-136V	540A	KDH12121E	
Drivetrain Specifications			
Gear Ratio	Chain Size	O-Rings	
53/16T	428	No	

4 Race Results and Data Analysis

The motorcycle competed in two qualifying races, and one final race. The average speed increased slightly with each race, though only a subset of the final race data is shown in this section. A summary of the results is shown in

Table 3. The time- and distance-series data was used to validate the system and subsystem models.

The speed versus distance plot in Figure 19 shows that the model closely matches the real world data when “full throttle” was applied during the race. This helps validate the models derived in Section 2.2.

Table 3: Race results.

Parameter	Units	Model	Race	Error
Battery Energy	[kWh]	9.6	9.8	2%
Average Battery Power	[kW]	21	22	5%
Battery Energy/Distance	[Watt-hrs/km]	158	161	2%
Average Battery Current	[A]	-	240	-
Average Current to Left Motor	[A]	-	149	-
Average Current to Right Motor	[A]	-	142	-
Average Speed	[km/hr]	-	127.3	-
Maximum Speed	[km/hr]	148	155	5%
0 to 144 km/hr (z = 3.3)	[sec]	24	25	4%
Finishing Time	[mins]	-	28.58	-

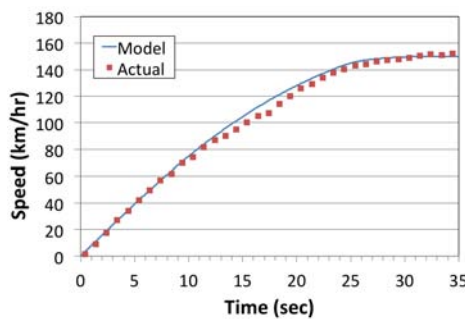


Figure 19: Speed data collected during the race.

The speed versus distance over the entire course is shown Figure 20. Each dip in the curve represents a corner in the course where the rider had to slow down. The speed data is shown with the corresponding altitude, which highlights the significant speed reduction while traversing up the mountain.

The power versus distance plot is shown in Figure 21, and it can be seen that the power fluctuates about a nominal value of ~ 22 kW. Plots were generated showing distance and energy versus time, and the linear nature of the curves showed that both constant speed and power were valid assumptions (plots are not

shown here). As predicted, analysis showed that the constant speed assumption underestimated the energy requirement, while constant power overestimated. An average of the energy consumed using both constant speed and power drive cycles matched the actual race data with $\sim 2\%$ error (Figure 22).

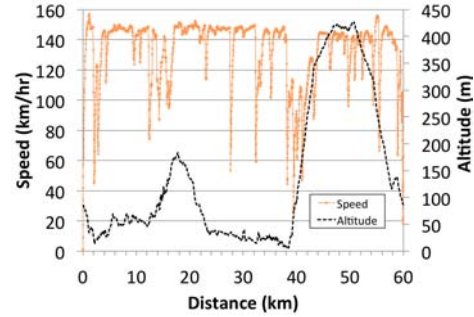


Figure 20: Speed data collected during the race.

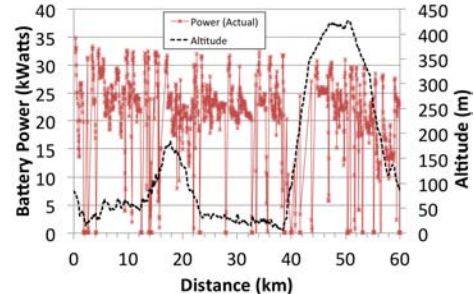


Figure 21: Power data collected during the race.

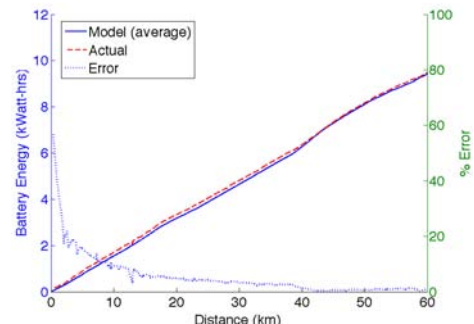


Figure 22: Actual (race) and predicted (model) values of battery energy consumed during the race.



Figure 23: The motorcycle during the TT race.

5 Electric Racing

The Isle of Man TT Zero is an example of a new breed of “zero emission” races. The aim of these races is to spur innovation that will reduce the environmental impact of consumer vehicles. Racing has historically been a catalyst for innovation, particularly in the early years of motorcycles and automobiles [8]. New concepts were tested on the track, and the desire to win drove companies to produce superior technology. Consumer demand for better performance motivated companies to transfer the technology from the race track to the mass market.

The fundamental question is whether or not zero emission racing will yield the desired outcome. With the goal of contributing to the success of zero emission racing, this section outlines a set of guidelines for designing zero emission races that will yield relevant innovation. In this paper innovation is defined as the act of generating a product or service that (1) reduces the environmental impact of vehicles and (2) consumers want to purchase.

5.1 Consider the historical context

Gasoline vehicle racing has evolved dramatically over the last 100 years. Because of this, caution should be used when copying a modern gasoline race with a zero emission equivalent. Zero emission racing might require a different approach, and lessons may be learned from looking back into the beginnings of gasoline racing.

Patience will also be required when directly comparing modern gasoline and zero emission racing. It is easy to forget that it took decades for gasoline engines to make dramatic improvements. For example, it took 50 years for the first gasoline motorcycle to reach a 100 mph average lap at the TT. The electric motorcycles will likely reach the same milestone within 5 years.

5.2 Utilize the power of regulation

Regulations should be used as the fundamental tool to engineer a race for a desired outcome. For example, assume that consumers want to refuel their vehicle quickly; if winning a zero emission race is dependent on fast refueling, then the regulations are successfully guiding development. A successful racing innovation platform must focus on technology relevant to the consumer market.

5.3 Drive technology

Many diverse participants, including inventors, academia, and corporate research labs, contribute to generating and developing innovative ideas. Consumer-focused companies choose relevant developments, refine them, and promote them to the consumer market. Identifying which ideas will succeed is a challenge facing all vehicle companies. Resources are often not available to invest in multiple emerging technologies. For example, it is costly for an automobile company to invest in batteries, fuel cells, and super capacitors simultaneously. Racing competitions should be structured to accelerate the transition from ideas to mass production and simultaneously facilitate the development of multiple technologies.

5.4 Provide valued entertainment

Any repeated event that the public finds entertaining will draw a large number of spectators both in person and through the media (e.g. internet, TV, etc.). Spectators and media drive advertising, which creates an influx of funds through team, rider and event sponsorship. These funds help finance the teams, who in turn develop the technology. Thus, valued entertainment is drawing in extra research and development funds *that would otherwise not be available for that purpose* (Figure 24). For example, an energy drink manufacturer might be indirectly funding battery research. This could translate into millions of dollars spent on zero emission innovation [9].

The influx of available sponsorship also reduces the risk that the team with the most personal wealth will win. In other words, sponsorships are typically chosen based on which team is likely to win; if the teams generating the most innovative vehicles are more likely to win, these teams would be rewarded through sponsorship funds to develop even better technology.

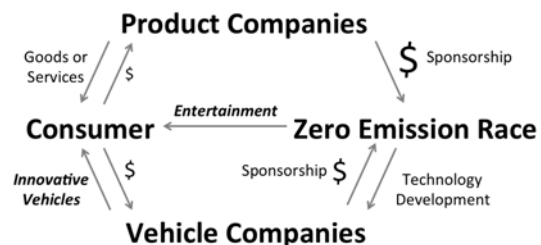


Figure 24: Valued entertainment can produce millions of dollars in research and development funds.

5.5 Inspire consumer demand

It is critical that the races inspire consumers to purchase the technology that is found superior on the race track. Otherwise, true innovation will not be achieved through racing, and the objective of reducing the environmental impact of vehicles will not be achieved. One way this can be accomplished is through styling, and ensuring that the race vehicle has brand identity. For example, a motorcycle company should use styling that is distinct and that connects their race vehicle to their commercially available vehicles.

Secondly, inspiration can be found through education. The race should strive to inform the consumer of the environmental effects and implications of the various technologies.

Finally, races can inspire consumer demand by building confidence in new technologies. For example, racing could prove that rapid charging is feasible, which might convince the skeptical consumer that the technology will satisfy their needs.

6 Conclusions

The design process consisted of systems engineering, subsystem design, final system design, testing, and model validation. Simulations were generated using a set of derived subsystem models. These simulations were useful for understanding how the design parameters affect performance metrics (Table 1). “Full throttle” simulations were performed to estimate the maximum acceleration, speed, and power of the motorcycle. To estimate the energy required to traverse the entire course, it is necessary to make assumptions about the throttle profile, power or speed. Since it was difficult to predict the throttle profile during the race, both constant speed and constant power drive cycles were assumed. It was found that an average of both drive cycles yielded accurate estimates of the energy consumed during the race (Figure 22).

Custom designs were generated for the instrumentation, motor shaft and structural frame that housed the motors and batteries. Special consideration was required when designing the structural frame, since the gasoline engine it replaced was previously a structural member (Figure 14). The unique design of the structural frame utilized a waterjet for fabrication, which allowed for easy prototyping and final fabrication (Figure 15). Real-time sensing provided a rich data set that was used to validate the system models (e.g. Figure 22); the models were able to

predict the acceleration, maximum speed, and energy consumption to within 5% of the actual values.

Finally, guidelines for designing innovative zero emission races were presented and described. In this paper innovation was defined as the act of generating a product or service that (1) reduces the environmental impact of vehicles and (2) consumers want to purchase. The guidelines suggest to consider the historical context, utilize the power of regulation, drive technology, provide valued entertainment, and inspire consumer demand.

Acknowledgments

This project would not have been possible without the generous support of A123 Systems, BMW, Singapore University of Technology and Design (SUTD), MIT-SUTD International Design Center (IDC), MIT Energy Initiative (MITEI), MIT Transportation, MIT Department of Mechanical Engineering, MIT School of Engineering, MIT Edgerton Center, the Isle of Man government, Dan Frey, Sanjay Sarma, and Mark Gardiner. And last but not least we would like to thank our professional and fearless rider Allan Brew and his wife Jan.

References

- [1] Honda Isle of Man TT Race Declaration, <http://world.honda.com/MotoGP/history/Man-TT-Declaration/>, accessed on 2012-01-13
- [2] Gardiner, M., *Riding Man*, ISBN 978-0979167300, Bike Writer Publishing, 2007
- [3] Rousseau, A., *Integrating Data, Performing Quality Assurance, and Validating the Vehicle Model for the 2004 Prius Using PSAT*, SAE International (SAE 2006-01-0667), 2006
- [4] Markel, T., *ADVISOR: a systems analysis tool for advanced vehicle modeling*, Journal of Power Sources, 2002
- [5] Cossalter, V., *Motorcycle Dynamics*, 2nd Edition, 2006
- [6] Guzzella, L., *Vehicle propulsion systems: introduction to modeling and optimization*, Springer, 2007
- [7] Ehsani, M., *Modern electric, hybrid electric, and fuel cell vehicles: fundamentals, theory, and design*, CRC Press, 2010
- [8] Frank, A., *Honda Motorcycles*, ISBN 0-7603-1077-7, MBI Publishing, 2003
- [9] Corbett, S., *NASCAR Sponsorship: Putting Your Company in the Driver’s Seat*, Journal of Integrated Communications, 2003

Table 4: Definitions of key variables.

Var.	Description
\ddot{x}	Acceleration of motorcycle
\dot{x}	Velocity of motorcycle
x	Position of motorcycle
t	Time
m	Mass of motorcycle and rider
z	Gear ratio times drivetrain efficiency
g	Gravity
C_{rr}	Rolling resistance coefficient
C_dA	Aerodynamic coefficient
β	Angle of road
w	Wind speed
F_w	Force from the rear wheel
P_w	Power from the rear wheel
τ_m	Motor torque
r_w	Radius of rear wheel
K_τ	Motor torque constant
K_θ	Motor back emf constant
R_m	Resistance of motor
$\dot{\theta}_m$	Rotational speed of motor
V_m	Voltage applied to motor
I_m	Current through motor
V_b	Battery pack voltage during discharge
I_b	Current from the battery pack
R_c	Internal resistance of a single cell
R_b	Internal resistance of the entire battery pack
k	Number of battery cell groups in series
l	Number of battery cells in parallel
I_m^{limit}	Current limit of motor controller
s	Throttle input from rider
V_b^n	Battery pack voltage when no current is flowing
P_b	Battery power
E_b	Battery energy
P_m	Motor power
η_d	Drivetrain efficiency
η_{mc}	Motor controller efficiency
\bar{x}	Average speed throughout the race
t_{finish}	Time to finish the race
X_{finish}	Distance of the race course
χ	Braking efficiency
\bar{x}^B	Average speed with braking
Δt^B	Time delay because of braking
t_{finish}^B	Time to finish with braking
E_b^B	Battery energy with braking

Authors

Lennon Rodgers is a PhD researcher at MIT, and is part of the MIT-SUTD International Design Center. He earned a B.S. from the University of Illinois Urbana/Champaign, and an M.S. from MIT. All of his degrees are in mechanical engineering. He worked for three years at Caltech and the Jet Propulsion Laboratory.



Radu Gogoana is a M.S. researcher at MIT and works in the Field Intelligence Lab. He earned undergraduate degrees in both mechanical engineering and business at MIT.



Thomas German is a Sloan Fellow at the MIT Sloan School of Management. Prior to MIT, he was the Penske Racing Technical Director for the NASCAR and IndyCar teams. Mr. German holds a B.S. in Mechanical Engineering from the University of Akron.

